

## Supporting Information

### Boosting selectivity towards formate production using CuAl alloy nanowires by altering the CO<sub>2</sub> reduction reaction pathway

Ibrahim M. Badawy<sup>a</sup>, Ghada E. Khedr<sup>a,b</sup>, Ahmed Hafez<sup>a</sup>, Elsayed A. Ashour<sup>c</sup>, Nageh K.

Allam<sup>a,\*</sup>

- a. Energy Materials Laboratory (EML), School of Sciences and Engineering, The American University in Cairo, New Cairo 11835, Egypt
- b. Department of Analysis and Evaluation, Egyptian Petroleum Research Institute, Cairo, 11727, Egypt
- c. Physical Chemistry Department, Advanced Materials Technology and Mineral Resources Research Institute, National Research Centre, Dokki 12622, Egypt

\* Corresponding Author's Email: [nageh.allam@aucegypt.edu](mailto:nageh.allam@aucegypt.edu)

### Table of Contents

Experimental synthesis and methods.....	S2
Phase diagram .....	S3
Additional FESEM images:.....	S4
XPS/XRD data tables and EDX mapping.....	S5
EIS measurements:.....	S6
Tabulated faradic efficiencies.....	S9
DFT further data and schematics: .....	S10
Experimental set-ups and FE calculation: .....	S13
Calibration curves and sample measurements .....	S14
Comparison with Literature .....	S15

## Experimental synthesis and methods

The Cu sheet (0.25 mm, 99.95%) was purchased from Alfa Aesar and used as is. The CuAl sheets were purchased from Goodfellow (1 mm, Cu91/Al9) and used as is. The copper nanowires were prepared through a well-established ammonium persulfate ((NH<sub>4</sub>)<sub>2</sub>S<sub>2</sub>O<sub>8</sub>, 98+%, Alfa Aesar) and sodium hydroxide (NaOH, ≥ 98%, Sigma Aldrich) etching method<sup>49,50</sup>. A solution of 0.1 M of (NH<sub>4</sub>)<sub>2</sub>S<sub>2</sub>O<sub>8</sub> and 1.2 M of NaOH was prepared where the copper sheets were gently submerged inside. The solution was kept between 10-15°C during the full etching time. Prior to the etching process, the metal foils were sanded using 1500 grit sandpaper, sonicated for 3 minutes in 10% v/v hydrochloric acid (HCl, Alfa Aesar) followed by deionized water (DI), ethanol (96%, Merck), and acetone (Merck) rinse. Kapton tape was used to mask the back of the metal foil. The CuAl nanowires were prepared through the exact same method. All nanowire samples were reduced in 0.1 M potassium bicarbonate (KHCO<sub>3</sub>, 99.5%, Chem Lab) saturated CO<sub>2</sub> (99.999%) electrolyte at 1.25 V vs Ag/AgCl for 10 min.

The electrochemical experiments were carried out in an acrylic H-type cell with two compartments separated by a proton exchange membrane (Nafion 117). The system involved gas-lines that were connected directly into the acrylic cell and lead out to the gas chromatography (GC). The purging gas, whether CO<sub>2</sub> (99.999%) CO (99.999%) or N<sub>2</sub> (99.9999%), was constantly running throughout the experiment at a fixed flow rate of 15 mL/min. A Biologic SP300 type potentiostat/galvanostat was used for all electrochemical experiments with a 3-electrode set-up in the acrylic cell. The counter electrode used was a platinized titanium mesh while the reference electrode was Ag/AgCl (KCl sat.). Unless otherwise stated, the electrolyte used for all measurements was aqueous 0.1 M KHCO<sub>3</sub> for both the cathode and anode compartments, which was bubbled. The measured potentials were converted to the reversible hydrogen electrode (RHE) reference scale using the formula.  $E_{RHE} = E_{Ag/AgCl} + 0.210 \text{ V} + 0.059 \text{ pH}$ . All currents were normalized to the geometric surface area of the electrodes. The pH of the electrolyte was measured to be 6.8. During the experiments, the gas phase products were quantified by a gas chromatography (SRI 8610C Multi-gas #5, 6' Haysep D and 6' Molecular Sieve 5A). The gas chromatography was equipped with a thermal couple detector (TCD), and a flame ionization detector (FID) with Argon (99.9999%) applied as the carrier gas. The liquid phase products were quantified using two different High-Performance Liquid Chromatography set-ups. For the formate detection Hypersil™ BDS C8 column was employed with a slightly acidified mobile phase and UV detector (220 nm). As for the alcohol detection, the NUCLEOSIL Thermo column was used along with the Refractive Index Detector (RID) and pure deionized water as the mobile phase.

### Materials characterization

The morphology of the samples was characterized by Zeiss SEM Ultra 60 field emission scanning electron microscope (FESEM) with 8 kV applied voltage. Rigaku SmartLab X-ray diffractometer was used to record the grazing incident x-ray diffraction (GIXRD) spectra in the 2θ range of 16°–90° at step rate of 0.2° at a grazing angle of 3°. X-ray diffraction (XRD) was also performed using the same range and step rate. As for the chemical composition, XPS measurements was performed using Thermo Scientific K-alpha+ XPS system. The system is equipped with Al-Kα monochromator X-ray source, with source operating power of 72 W. The survey scans were conducted at a pass energy of 200 eV, while high-resolution scans were conducted at 50 eV pass energy. To eliminate shift of binding energies from surface charging, flood gun source was activated during the scan. Measurement spot size used during measurements was 400 μm. For

analysis, high-resolution spectra were resolved by fitting the peaks using Gaussian-Lorentzian function combination after background subtraction. The atomic concentrations were calculated by normalizing the areas under fitted peaks. Attenuated Total Reflection Fourier Transform Infrared Spectroscopy (ATR-FTIR, Thermo-Fisher Scientific, USA) was performed on the electrocatalyst samples using a Silicon lens.

### Computational details

Binding energies of the intermediates and transition states on Cu<sub>2</sub>O (111) surface and Cu<sub>2</sub>O with 7% Al (111) were calculated using Vienna Ab initio Simulation Package (VASP) software with Vanderbilt ultrasoft pseudopotentials. A supercell of 2×2×1 was created. A vacuum slab of 15 Å was built to prevent interaction with their periodic images. The supercell consists of four layers and the two upper layers are relaxed and the two bottom layers are fixed. The generalized gradient approximation (GGA) with Perdew–Burke–Ernzerhof (PBE) function were used with cut-off energy 440 eV, self-consistent field (SCF) tolerance of  $1.0 \times 10^{-8}$  eV. The Brillouin zone was sampled with a Monkhorst–Pack k-point of 4×4×1. For relaxation, we used conjugate gradient (CG) algorithm. Transition states were calculated for C-C dimer and C-O bond dissociation using climbing image nudged elastic band method (NEB). Transition states were confirmed by having only one negative frequency<sup>51</sup>. VASPsol software was used to investigate the water-solvent effect on all the intermediates. It is an implicit solvation model which is based on Polarizable Continuum Model (PCM).

### Phase diagram

The phase diagram of Cu-Al has many phases and is a complicated system. The figure shows a section for the phase diagram<sup>1</sup>. As can be observed the prepared sample is expected to lie between Cu<sub>4</sub>Al and Cu boundary line (90%, 180C), the XRD measurements however confirm the sample is mostly a single phase where the Al is in solid solution with the Cu.

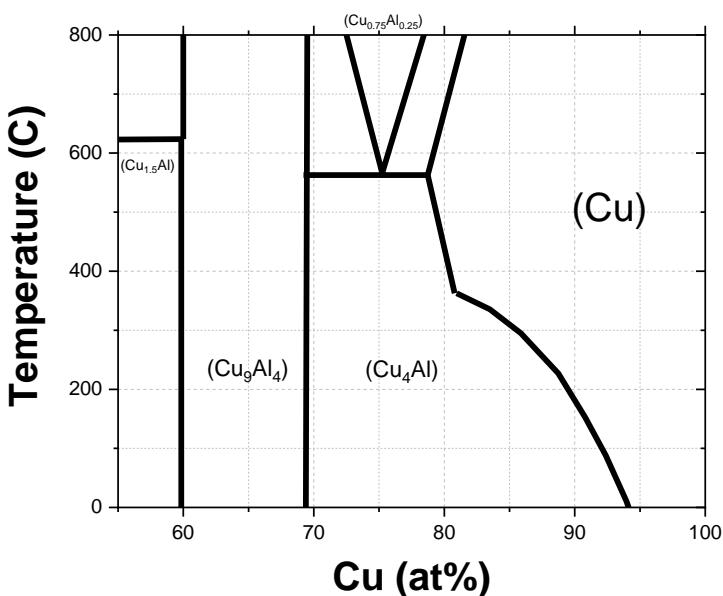


Figure S1. Sectioned phase diagram of Cu-Al

<sup>1</sup> Thermochemical Database for Light Metal Alloys, I. Ansara, European Commission, Directorate-General XII, Science, Research and Development, 1994

## Additional FESEM images:

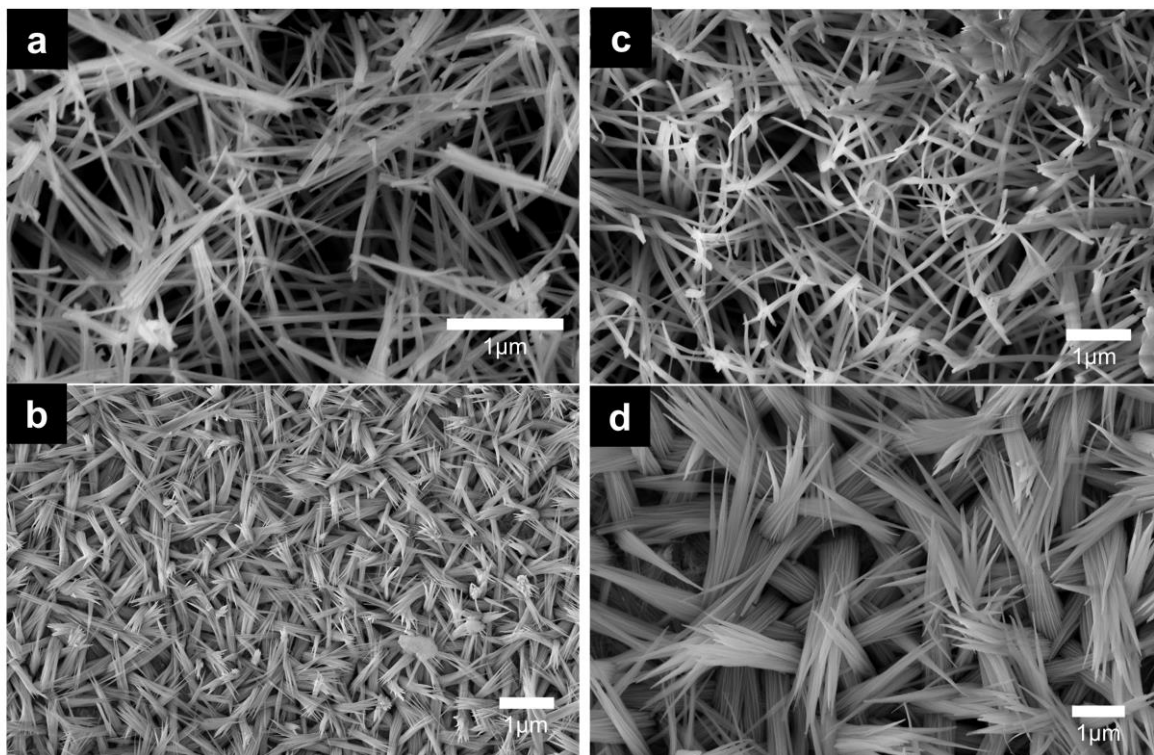


Figure S2. FESEM images of a) CuNW before annealing, b) CuAlNW before annealing, c) CuNW after annealing, d) CuAlNW after annealing

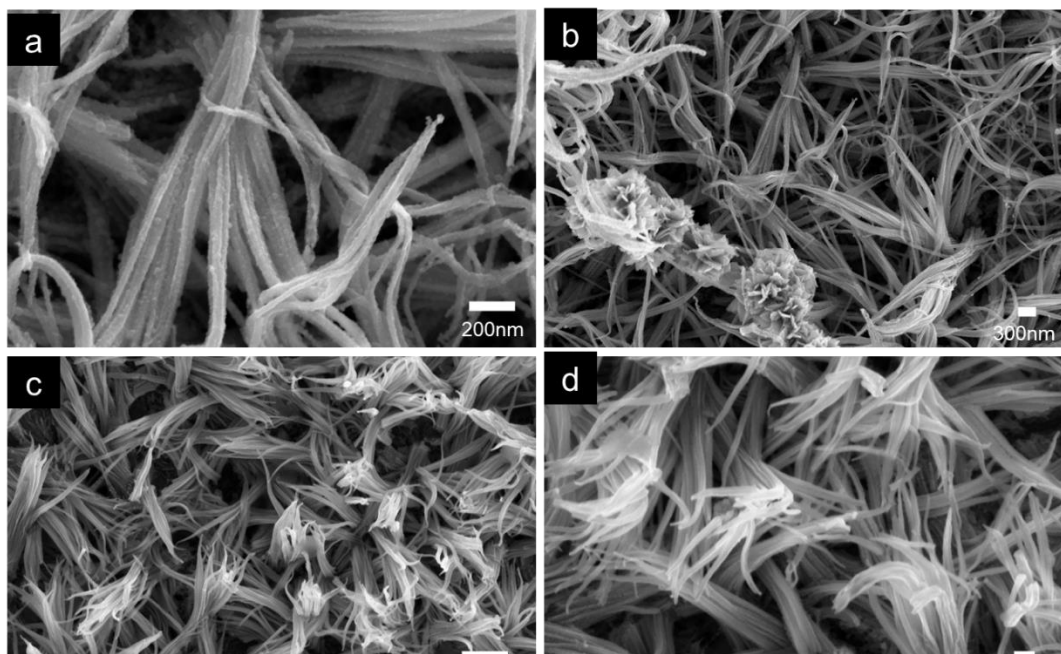


Figure S3. FESEM images of a) & b) CuNW and c) & d) CuAlNW after electrochemical CO<sub>2</sub>RR run

## XPS/XRD data tables and EDX mapping

Table S1. Quantification of elements in CuAl alloy using different instruments

Method of analysis	Cu	Al
XPS	88.73%	11.72%
EDX	90.85%	9.15%

Table S2. Extracted XRD data from diffractograms

Sample	Peak pos. ( $^{\circ}2\theta$ )	(hkl)	FWHM	Crystallite size ( $\text{\AA}$ )	Lattice strain (%)
CuNW	43.338	(111)	0.116	743	0.127
	50.463	(002)	0.160	552	0.148
	74.108	(022)	0.260	384	0.15
CuAlNW	42.673	(111)	0.440	194	0.491
	49.701	(002)	0.400	219	0.377
	72.979	(022)	0.840	118	0.496

Table S3. Relative measured XPS quantities of CuAl alloy under different conditions

Sample	Cu	Al	Al <sub>2</sub> O <sub>3</sub>
CuAl	88.73%	11.27%	-
CuAlNW	82.24%	2.07%	15.69%
CuAlNW after CO <sub>2</sub> R run	85.45%	5.33%	9.22%

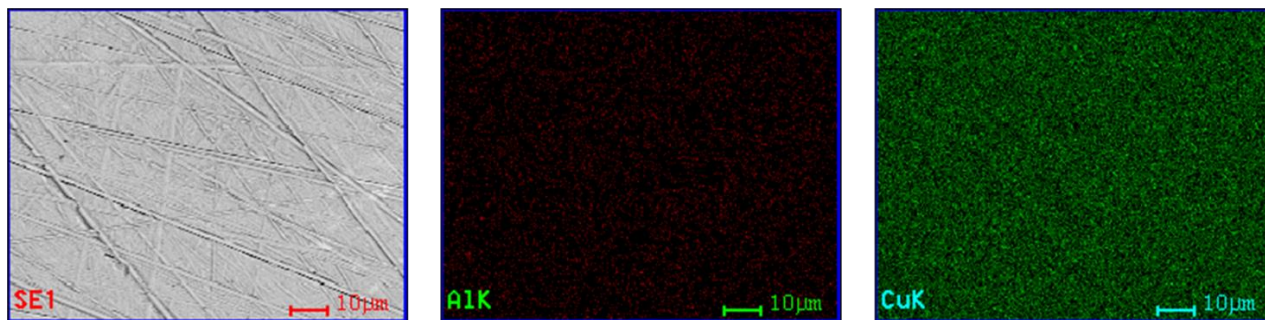


Figure S4. EDX mapping of CuAl alloy sample

## EIS measurements:

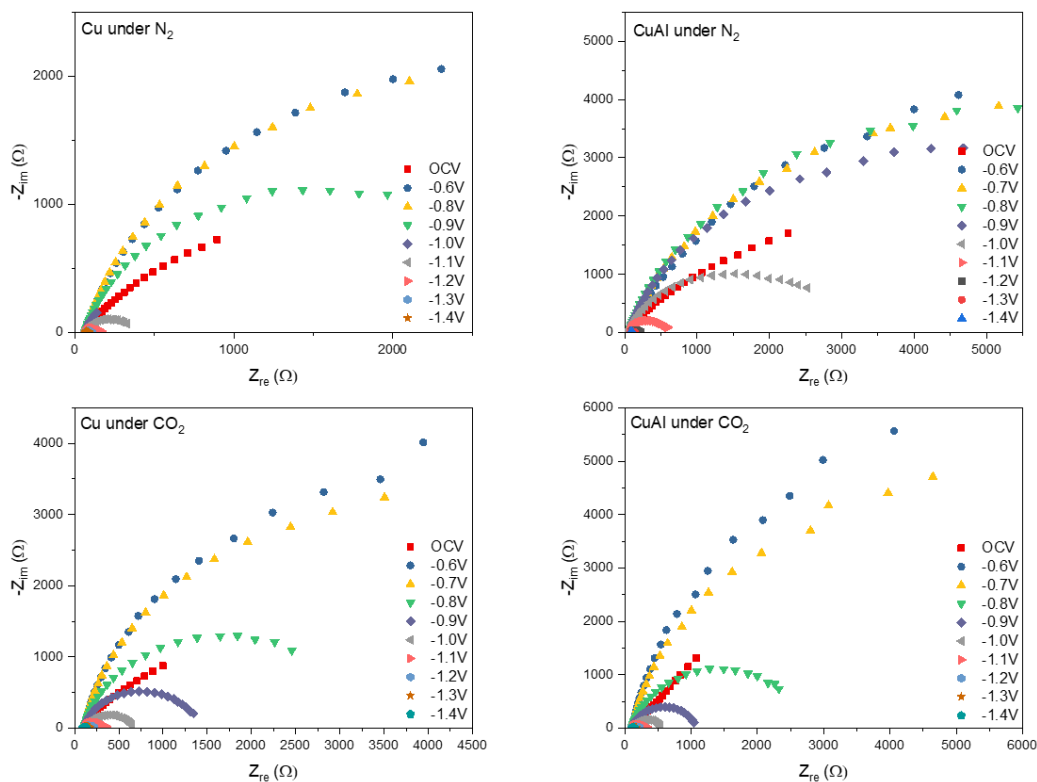


Figure S5. Nyquist plots for all the potentials tested vs Ag/AgCl.

The EIS measurements were conducted under two main conditions: 0.1M  $\text{KHCO}_3$  under  $\text{CO}_2$  purge and 0.1M  $\text{Na}_2\text{SO}_4$  (Sigma Aldrich, 99.999%) under  $\text{N}_2$  (99.999%) purge as specified in the figure. The Nafion membrane was allowed to soak for 24h in the corresponding electrolyte before the day of the measurement. The measurements were conducted in sequence with a 12min relaxation time at OCV between each measurement. The circuit model result presented below were extracted and modelled using Biologic's built in software.

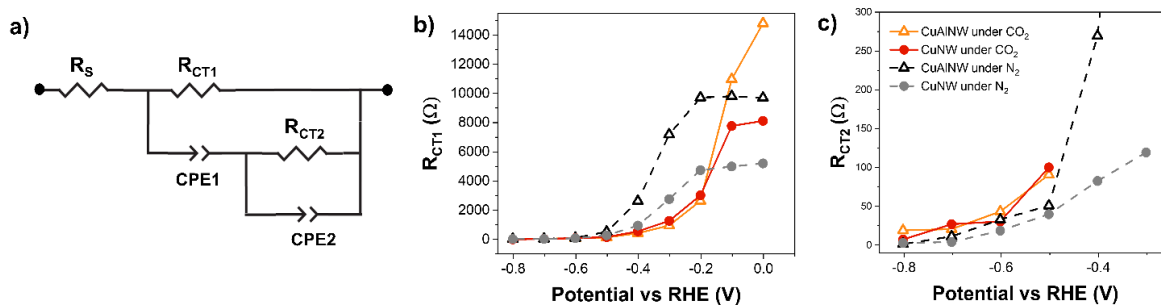


Figure S6. EIS measurements between 0V to -0.8V vs RHE of CuNW and CuAlNW under  $\text{CO}_2$  purge and  $\text{N}_2$  purge with a) the fitted model circuit and the values of the charge transfer resistor components b)  $R_{CT1}$  and c)  $R_{CT2}$

EIS was performed at a range of potentials under CO<sub>2</sub>R conditions and under non-CO<sub>2</sub>R conditions (under N<sub>2</sub> purge) to investigate the electrochemical interface, i.e. electrode-electrolyte interface. The Nyquist plots, presented in Supplementary Figure 7, are fitted to a model with two embedded parallel R||C circuits to account for two semicircle arcs observed at >-0.5V vs RHE and a single semicircle at <-0.5V vs RHE. The model can be seen in Figure 3a. This type of model is typically invoked to describe the contact resistance between the surface passivation, the bulk, and the electrode-electrolyte interface. The XPS findings corroborate this model where the charge-transfer resistor (R<sub>CT</sub>) components represent these interfaces. In Figure 3c,d, CuAlNW under N<sub>2</sub> shows relatively large resistances at <-0.5V vs RHE for both R<sub>CT</sub> components, indicating a strong passivation layer that is likely caused by the Al<sub>2</sub>O<sub>3</sub> formed on the surface. The resistance decreases sharply however and equalizes with the rest of the samples at >-0.5V vs RHE. CuNW also appears to have a CuO passivation layer that fades with the increasing reduction potential. These observations are important to later model the system computationally using DFT, where the reduced alloy is the form in which the electrodes are reacting.

Table S4. Component values of the model circuit at the measured potentials

	N <sub>2</sub>							CO <sub>2</sub>					
	V vs RHE	Q1/ F.s <sup>α-1</sup>	α1	R1/Ω	Q2/F.s <sup>α-1</sup>	α2	R2/Ω	Q1/ F.s <sup>α-1</sup>	α1	R1/Ω	Q2/F.s <sup>α-1</sup>	α2	R2/Ω
<b>CuAINW</b>	0	1.14E-03	0.8580	9700	–	–	–	1.08E-03	0.912	14808	–	–	–
	-0.1	9.77E-04	0.8638	9807	–	–	–	1.24E-03	0.9068	10977	–	–	–
	-0.2	9.43E-04	0.8639	9722	–	–	–	1.49E-03	0.8817	2641	–	–	–
	-0.3	9.93E-04	0.8445	7189	0.01102	1	853.7	1.26E-03	0.8768	956.7	–	–	–
	-0.4	1.04E-03	0.8298	2630	0.03433	1	269.5	1.33E-03	0.8298	429.1	–	–	–
	-0.5	1.06E-03	0.8547	522.8	0.07466	1	50.98	9.62E-04	0.9347	139.9	0.01805	0.7943	90.68
	-0.6	1.91E-03	0.8941	107.4	0.07687	0.6294	32.96	1.43E-03	0.8612	77.55	0.06459	0.8787	43.33
	-0.7	1.06E-03	0.9118	43.51	0.2326	0.6939	11.2	1.28E-03	0.8596	50.14	0.1324	0.8372	20.68
	-0.8	8.02E-04	0.9382	26.03	0.4624	1	1.395	1.22E-03	0.8914	32.81	0.1841	0.7033	19.03
<b>CuNW</b>	0	2.46E-03	0.8515	5210	–	–	–	1.69E-03	0.9118	8122	–	–	–
	-0.1	2.64E-03	0.8421	4987	–	–	–	1.96E-03	0.9087	7772	–	–	–
	-0.2	2.90E-03	0.8725	4748	–	–	–	2.15E-03	0.9384	3023	–	–	–
	-0.3	2.35E-03	0.8515	2762	0.1211	1	119.4	1.44E-03	0.8817	1276	–	–	–
	-0.4	2.22E-03	0.8383	950.3	0.07853	1	82.53	1.90E-03	0.7415	551.7	–	–	–
	-0.5	2.62E-03	0.8198	283.7	0.1492	1	39.81	1.17E-03	0.9301	156.1	0.01181	0.6624	100.1
	-0.6	3.14E-03	0.8509	82.87	0.3185	1	18.69	1.99E-03	0.8289	87.89	0.06441	0.861	30.56
	-0.7	3.13E-03	0.8476	37.75	0.7346	0.8825	4.018	1.36E-03	0.9089	42.67	0.02568	0.5391	27.01
	-0.8	2.49E-03	0.8876	21.6	0.995	0.7144	2.812	2.04E-03	0.8491	5.24	0.1137	0.8851	7.288

## Tabulated faradic efficiencies

Table S5. Faradic efficiencies measured for CuNW at the different tested potentials

Potential (V vs RHE)	H <sub>2</sub>		CO		CH <sub>4</sub>		C <sub>2</sub> H <sub>4</sub>		C <sub>2</sub> H <sub>6</sub>		CHOO <sup>-</sup>	
-0.7	0.768	0.122	0.081	0.011	0	0	0	0	0	0	0.113	0.037
-0.8	0.807	0.009	0.038	0.009	0	0	0.061	0.009	0.011	0.011	0.151	0.045
-0.9	0.783	0.026	0.036	0.011	0	0	0.109	0.054	0.035	0.005	0.107	0.021
-1.0	0.669	0.073	0.034	0.008	0	0	0.122	0.027	0.069	0.003	0.006	0.028

Table S6. Faradic efficiencies measured for CuAlNW at the different tested potentials

Potential (V vs RHE)	H <sub>2</sub>		CO		CH <sub>4</sub>		C <sub>2</sub> H <sub>4</sub>		C <sub>2</sub> H <sub>6</sub>		CHOO <sup>-</sup>	
-0.7	0.412	0.041	0.049	0.009	0	0	0	0	0	0	0.282	0.0094
-0.8	0.491	0.035	0.103	0.008	0	0	0.065	0.013	0	0	0.206	0.044
-0.9	0.437	0.092	0.075	0.012	0	0	0.030	0.004	0	0	0.114	9.30E-04
-1.0	0.658	0.045	0.031	0.001	0	0	0.036	0.003	0	0	0.102	0.026

## DFT further data and schematics:

The free CO<sub>2</sub> molecule was optimized in a 10×10×10 Å<sup>3</sup> unit cell. The optimized C–O bond length and O–C–O angle are 1.178 Å and 180.0°, respectively, which are matched with the available experimental and theoretical data. The adsorption energy of CO<sub>2</sub> is calculated as follows:

$$E_{\text{ads}} = E_{\text{CO}_2+\text{surface}} - [E_{\text{CO}_2} + E_{\text{surface}}]$$

where  $E_{\text{CO}_2+\text{surface}}$  represents the energy of the surface with the adsorbed CO<sub>2</sub>,  $E_{\text{CO}_2}$  represents the energy of free CO<sub>2</sub>, and  $E_{\text{surface}}$  represents the energy of the surface. The Cu site was chosen for adsorption. Adsorption energies were calculated relative to H<sub>2</sub>(g) as

$$\Delta E = E_{\text{slab+H}} - E_{\text{slab}} - \frac{1}{2}E_{\text{H}_2}$$

The associated free energy of H is

$$\Delta G = \Delta E + \Delta \text{ZPE} - T\Delta S$$

$\Delta \text{ZPE}$  being the difference in zero-point energy and  $\Delta S$  the difference in entropy between the adsorbed state and gas phase. Since  $\Delta \text{ZPE} - T\Delta S \approx 0.24$  eV. We have  $\Delta G = \Delta E + 0.24$  eV.

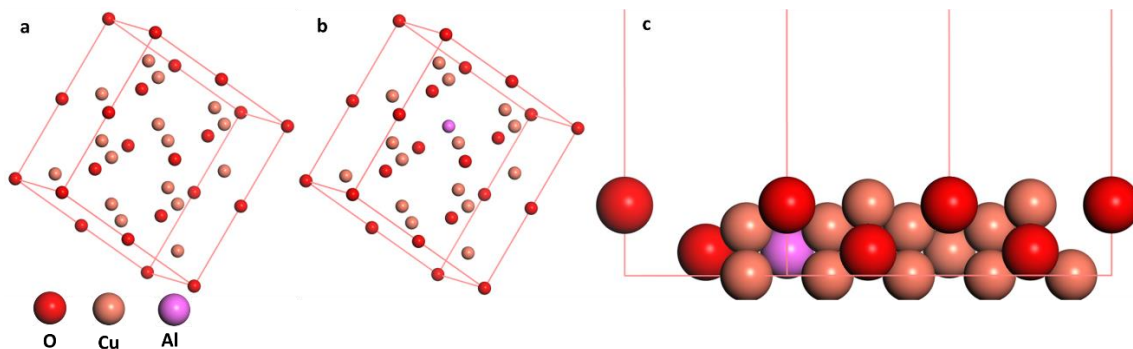


Figure S7. Optimized geometries for a) Cu<sub>2</sub>O bulk b) Cu<sub>2</sub>O with 7% Aluminum c) Cu<sub>2</sub>O with 7% Aluminum (111) surface

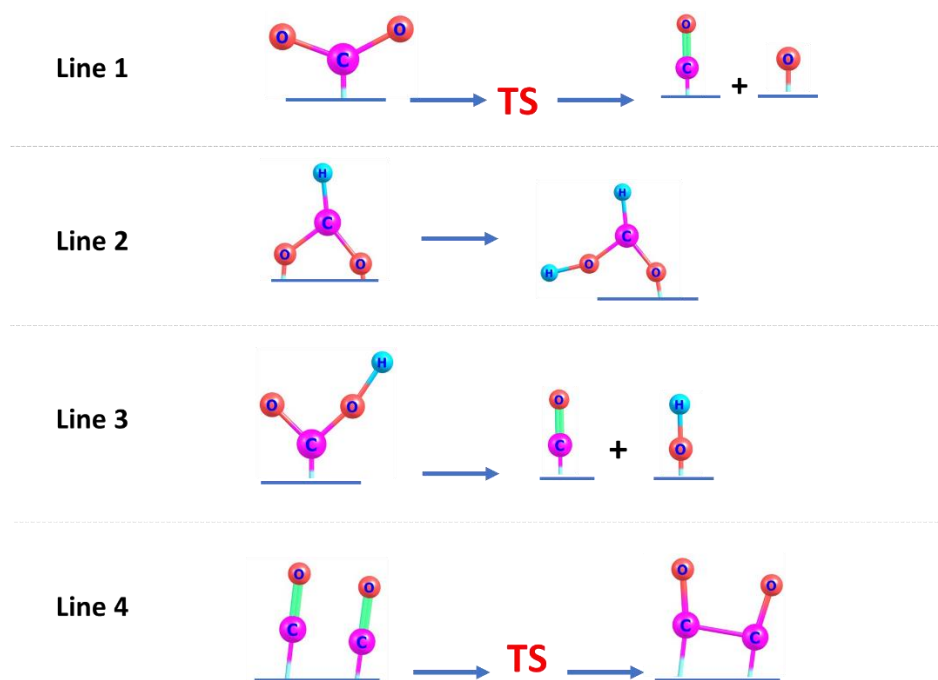


Figure S8. Schematic of the 4 reaction pathways posited for the reduction of CO<sub>2</sub> on the surface catalysts

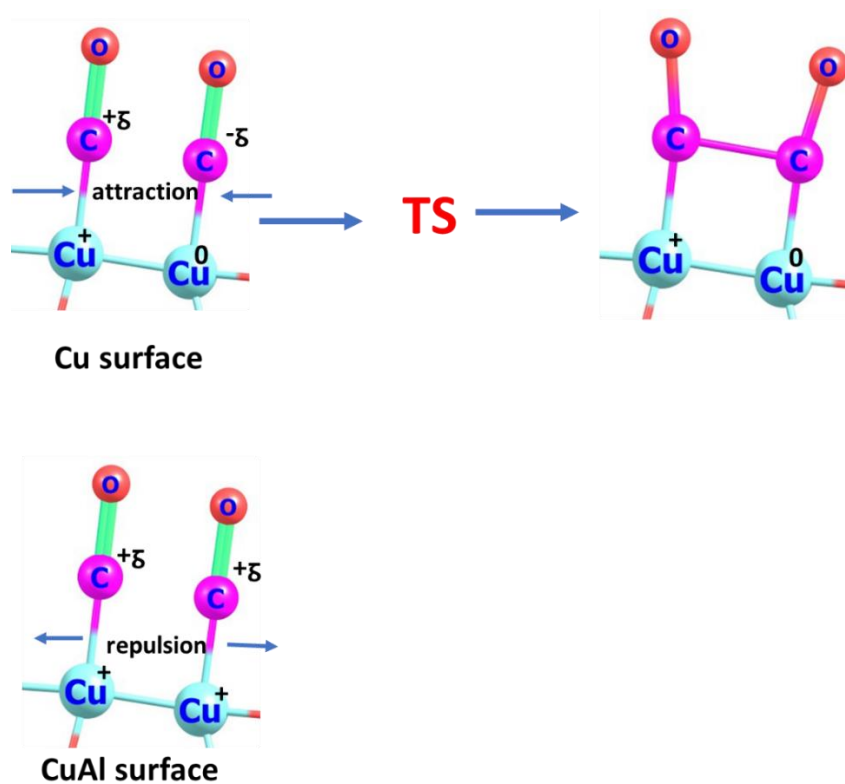


Figure S9. Proposed mechanism for C-C dimerization on Cu and CuAl surface

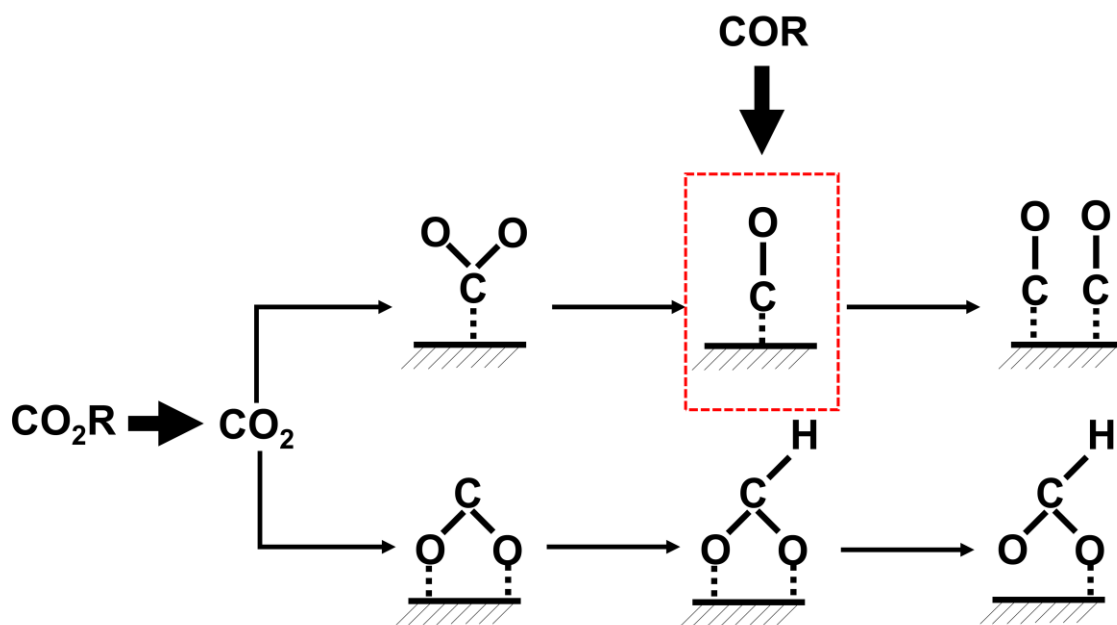


Figure S10. Theorized entry point of COR in the  $\text{CO}_2\text{R}$  reaction pathway

## Experimental set-ups and FE calculation:

The H-cell used to conduct the CO<sub>2</sub>R experimental runs was inspired from Dr Kuhl's design. It consists of two acrylic plates each fitted with 8x8mm working area where the anode and cathode materials are placed. Nafion 117 membrane is sandwiched between the two plates. A hole is made in the cathode compartment where the reference electrode is placed as seen in below. CO<sub>2</sub> (99.999%) gas is made to flow through the h-cell from the bottom-up at a controlled rate of 15sccm using a mass flow controller (MFC). The outlet of the H-cell is directed towards the inlet valve of the GC where product gas is analyzed at the following set times: 13mins, 32mins, 55mins, 70mins. The total runtime for each run was 72mins.

As for the COR experiments, they were carried out in the fume hood as shown in the figure below. 0.1M KOH purged with CO (99.999%) was used as the electrolyte. The total run time of the experiment was shortened to 30mins and only the gas products were detected and analyzed. The CO gas was allowed to continue flowing at a rate of 15 sccm throughout the duration of the experiment. Because the electrolyte is basic a Hg/HgO reference electrode was used to give a more accurate measurement of the potential. The applied potentials were corrected accordingly.

The FE for gas and liquid products were calculated using the following equation:

$$FE (\%) = \frac{nN_p F}{\int_0^t i dt} \times 100$$

where n is the stoichiometric coefficient of the electron for the reaction (n=2 for CO, HCOOH). N<sub>p</sub> is the amount in moles of the product measured by the GC or HPLC. F is the faraday constant of 96,485 Cmol<sup>-1</sup>. The current is indicated as i in amperes and t is the time in seconds.

The partial current was calculated according the following equation:

$$j_p = FE_p \times i_{tot}$$

where FE<sub>p</sub> is the faradic efficiency for the selected product and i<sub>tot</sub> is the total current measured for that time.

## Calibration curves and sample measurements

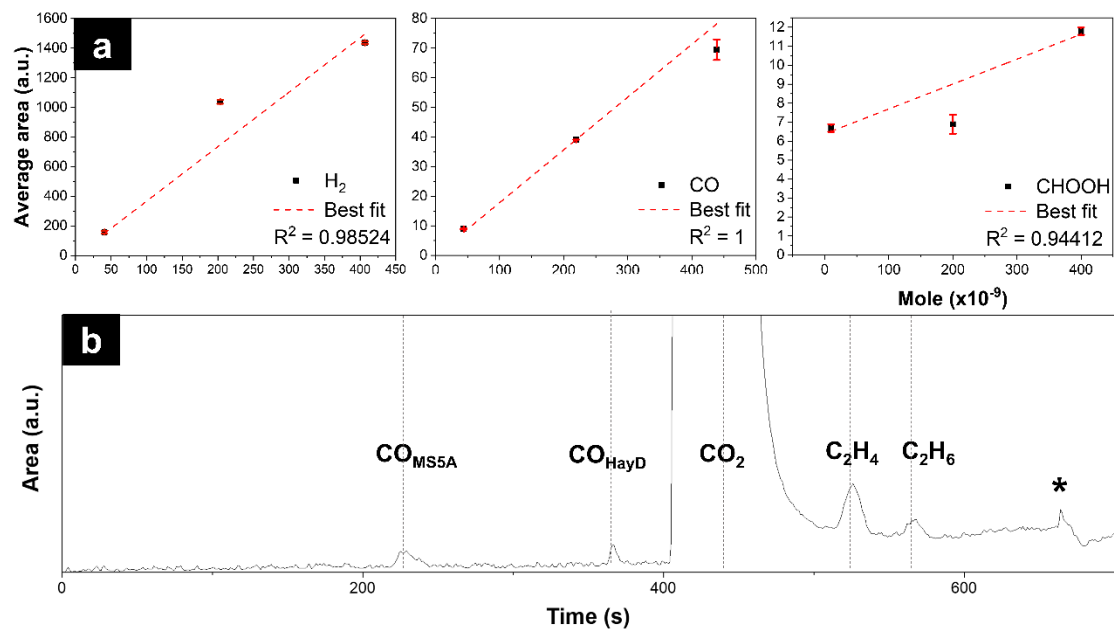


Figure S11.a) Sample calibration curves with b) sample GC measurement \*valve change

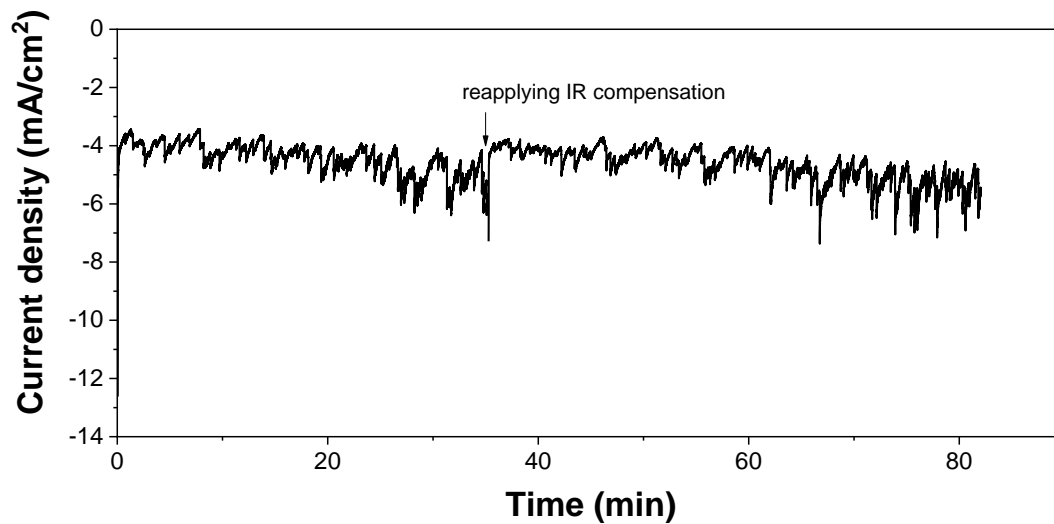


Figure S12. Sample chronoamperometry run for CuAlNW that demonstrates the electrocatalyst stability after 82mins at -0.9V vs RHE

## Comparison with Literature

Table S7. Comparison of FE of formate with the most relevant literature

Material	Electrolyte	Cell type	Potential vs RHE	FE of formate	Reference
Ga-doped CuAl ( $\approx 50\%$ Al)	1M KHCO <sub>3</sub>	H-cell	-1.4V	10.3%	A. Sedighian Rasouli, X. Wang, J. Wicks, C. T. Dinh, J. Abed, F. Y. Wu, S. F. Hung, K. Bertens, J. E. Huang and E. H. Sargent, <i>Chem Catal.</i> , 2022, <b>2</b> , 908–916.
CuO/Al <sub>2</sub> CuO <sub>4</sub> (15.54% Al)	0.1M KHCO <sub>3</sub>	H-cell	-0.99V	$\approx 8\%$	S. Sultan, H. Lee, S. Park, M. M. Kim, A. Yoon, H. Choi, T. H. Kong, Y. J. Koe, H. S. Oh, Z. Lee, H. Kim, W. Kim and Y. Kwon, <i>Energy Environ. Sci.</i> , 2022, <b>15</b> , 2397–2409.
Cu <sub>80</sub> Al <sub>20</sub>	1M KHCO <sub>3</sub>	Flow-cell	-0.92V	$\approx 5\%$	R. S. Kanase, K. B. Lee, M. Arunachalam, R. P. Sivasankaran, J. Oh and S. H. Kang, <i>Appl. Surf. Sci.</i> , 2022, <b>584</b> , 152518.
CuAlNW	0.1M KHCO <sub>3</sub>	H-cell	-0.7V	28.2 $\pm$ 0.94%	This work